



Since January 2020 Elsevier has created a COVID-19 resource centre with free information in English and Mandarin on the novel coronavirus COVID-19. The COVID-19 resource centre is hosted on Elsevier Connect, the company's public news and information website.

Elsevier hereby grants permission to make all its COVID-19-related research that is available on the COVID-19 resource centre - including this research content - immediately available in PubMed Central and other publicly funded repositories, such as the WHO COVID database with rights for unrestricted research re-use and analyses in any form or by any means with acknowledgement of the original source. These permissions are granted for free by Elsevier for as long as the COVID-19 resource centre remains active.



Early chest computed tomography to diagnose COVID-19 from suspected patients: A multicenter retrospective study

Congliang Miao, MD^{a,1}, Mengdi Jin, MD^{b,1}, Li Miao, MA^c, Xinying Yang, MD^d, Peng Huang, MD^e, Huanwen Xiong, MD^c, Peijie Huang, MD^a, Qi Zhao, MD^a, Jiang Du, MD, PhD^{a,*}, Jiang Hong, MD, PhD^{a,*}

^a Department of Internal and Emergency Medicine, Shanghai General Hospital, Shanghai Jiao Tong University, Shanghai 201600, China

^b Department of Internal and Emergency Medicine, Shanghai General Hospital, Shanghai Jiao Tong University School of Medicine, Shanghai 201600, China.

^c Department of Respiratory Diseases, High-tech Hospital, First Hospital Affiliated to Nanchang University, Jiangxi 330000, China

^d Department of Internal and Emergency Medicine, Shanghai General Hospital of Nanjing Medical University, Shanghai 201600, China

^e Department of Infectious Diseases, People's Hospital of Yichun city, Jiangxi 336000, China.

ARTICLE INFO

Article history:

Received 18 March 2020

Received in revised form 14 April 2020

Accepted 14 April 2020

Keywords:

Coronavirus infections

Viral pneumonia

Computed tomography

Sensitivity and specificity

Reverse-transcription polymerase chain reaction

China

ABSTRACT

Objective: The purpose of this study was to distinguish the imaging features of COVID-19 from those of other infectious pulmonary diseases and evaluate the diagnostic value of chest CT for suspected COVID-19 patients.

Methods: Adult patients suspected of COVID-19 aged >18 years who underwent chest CT scans and reverse-transcription polymerase chain reaction (RT-PCR) tests within 14 days of symptom onset were enrolled. The enrolled patients were confirmed and grouped according to the results of the RT-PCR tests. The basic demographics, single chest CT features, and combined chest CT features were analyzed for the confirmed and nonconfirmed groups.

Results: A total of 130 patients were enrolled, with 54 testing positive and 76 testing negative. The typical CT imaging features of the positive group were ground glass opacities (GGOs), the crazy-paving pattern and air bronchogram. The lesions were mostly distributed bilaterally and close to the lower lungs or the pleura. When features were combined, GGOs with bilateral pulmonary distribution and GGOs with pleural distribution were more common among the positive patients, found in 31 (57.4%) and 30 patients (55.6%), respectively. The combinations were almost all statistically significant ($P < .05$), except for the combination of GGOs with consolidation. Most combinations presented relatively low sensitivity but extremely high specificity. The average specificity of these combinations was approximately 90%.

Conclusions: The combinations with GGOs could be useful in the identification and differential diagnosis of COVID-19, alerting clinicians to isolate patients for prompt treatment and repeat RT-PCR tests until the end of incubation.

© 2018 Elsevier Inc. All rights reserved.

1. Introduction

An outbreak of unexplained pneumonia occurred in Wuhan City, Hubei Province, China, in December 2019 [1]. The virus causing the epidemic was detected as a new coronavirus (2019-nCoV), and the resulting pneumonia was then named by the WHO as Coronavirus Disease 2019 (COVID-19) [2–4]. As of March 17, 2020, a total of 81,118

Abbreviations: 2019-nCoV, 2019 novel coronavirus; COVID-19, Coronavirus Disease 2019; RT-PCR, reverse-transcription polymerase chain reaction; HRCT, High-resolution computed tomography; GGO, ground glass opacity; MERS, Middle East respiratory syndrome; SARS, Severe acute respiratory syndrome; BALF, Bronchoalveolar lavage fluid.

* Corresponding authors at: Department of Internal and Emergency Medicine, Shanghai General Hospital, Shanghai Jiao Tong University, Xinsongjiang Road 650, Shanghai 201600, China.

E-mail addresses: gowindj@163.com (J. Du), jhong.pku@163.com (J. Hong).

¹ Contributed equally to this work.

patients in China have been diagnosed with confirmed COVID-19, and 68,802 patients were cured and discharged [5]. At the same time, the number of suspected cases has also decreased significantly. This shows that China's epidemic prevention policy has achieved initial results. However, the infection has spread to over 48 countries worldwide, especially in Iran, Korea and some European countries, even affecting the United States. The global risk of this epidemic was escalated to the highest level by the WHO on February 28. Fast and effective diagnostic methods for this disease are of great importance at present.

According to the latest Diagnosis and Treatment Program for COVID-19 of China [6], the diagnosis of COVID-19 requires a reverse-transcription polymerase chain reaction (RT-PCR) test, but a certain rate of false negative results has been reported [7]. Its limited production and relatively long testing period might not be conducive for screening. Accumulated clinical experience suggests that early chest computed tomography might be helpful in the differential diagnosis of

suspected cases. Recently, Chung, Fang and Kanne, etc. reported the chest CT imaging features of COVID-19 [8–10]. Fang and Ai further studied the sensitivity of chest CT compared to RT-PCR with a relatively small sample [9,11]. However, there is no agreed standard for how to confirm a diagnosis of COVID-19 with these features. We retrospectively collected chest CT images of suspected pneumonia patients, divided them according to the results of RT-PCR tests into positive and negative groups and then compared the differences in CT features between the two groups. Our goal is to use statistical methods to distinguish the imaging features of COVID-19 from other infectious pulmonary diseases and evaluate the diagnostic value of chest CT for suspected COVID-19 patients.

2. Materials and methods

2.1. Patient population

The data used in this multicenter retrospective study were collected from three tertiary hospitals of two provinces in China. We enrolled a consecutive sample of suspected COVID-19 patients from January 12, 2020 to February 13, 2020 according to the following inclusion criteria: (1) suspicion of COVID-19 according to the 6th edition of the Diagnosis and Treatment Program for COVID-19 of China [6]; (2) age over 18 years; and (3) <14 days from onset to first CT. Exclusion criteria included (1) past history of chronic lung disease and (2) pregnancy. Finally, 130 patients participated in our research. These patients' general information, epidemiological history and CT imaging data were retrospectively collected.

2.2. Study design

The diagnostic criteria for suspected cases are as defined in the 6th edition of the Diagnosis and Treatment Program for COVID-19 of China [6]. Nasopharyngeal swabs or sputum specimens were collected for running RT-PCR tests. Patients with first negative results received repeated tests after an interval of at least 1 day. All suspected cases were divided into positive and negative groups according to the results of the RT-PCR test. Patients who were negative before but positive on retests were eventually defined as positive.

All patients were prepared for CT scan examination; 33 patients were scanned on an Optima 670 CT scanner, GE, 41 patients were scanned on Revolution Frontier, GE, and 56 patients were scanned on a SOMATOM Definition Flash, Japan. Examinations followed the normal chest protocols. The overall scan time was 2 s, and the slice thickness for reconstruction was 1.25 mm. All the reports were issued after double-blind reviews by two radiologists and were resolved by a chief radiologist when opinions diverged.

This study was approved by the Ethics of Committees of the local hospital. Informed consent for this retrospective study was waived.

2.3. Qualitative image analysis

According to the newly reported CT imaging features of COVID-19 and previous studies on the disease [12], we summarized the features that may appear on early chest CT. Lesion morphology was described as the presence of (1) a ground-glass opacities (GGOs); (2) consolidation; (3) crazy-paving pattern; (4) air bronchogram; (5) cavitation; (6) pulmonary nodule; (7) lymphadenopathy; (8) pleural effusion; (9) pulmonary atelectasis; or (10) pleural thickening. Lesion distribution, such as whether they were unilateral, bilateral or peripleural, the number of lung lobes involved and the involvement of the upper, middle, and lower fields of the lung were also counted.

2.4. Statistical analysis

Patient data were recorded by Epidata, and statistical analysis was performed using SPSS 13.0 (IBM Corporation). Normally distributed continuous variables are expressed as the mean \pm SD ($\bar{x} \pm s$), and variables with a skewed distribution were presented as the medians (interquartile ranges). Independent *t*-tests were used to compare measurement data, and Mann-Whitney *U* tests were used for data with skewed distributions. Categorical information is described by percentages and was compared using the chi-squared test or Fisher's exact test. All statistical tests were bidirectional comparisons, and $P < .05$ was regarded as statistically significant.

3. Results

3.1. Comparisons of basic demographics

A total of 166 patients were enrolled in this study. Excluding 2 patients younger than 18 years old, 28 patients with normal CT presentations, 2 patients with underlying lung disease, 2 patients with onset to consultation over 14 days, and 2 patients who could not undergo chest CT because of pregnancy, 130 patients were finally included in the statistical analysis, with 54 testing positive and 76 testing negative for COVID-19 (see Fig. 1). As shown in Table 1, the mean age of the positive group patients was 45.1 ± 13.4 years, ranging from 19 to 77 years, and 28 of the patients were males (51.9%). The average time from symptom onset to the first visit was 4 days. For the negative group patients, the average age was 41.8 ± 13.6 years, ranging from 19 to 81 years, and 49 of the patients were males (64.5%). The average time from the onset of symptoms to the first visit was 3 days. The proportion of patients with a history of Wuhan residence and the clustering incidence between the two groups were statistically significant ($P < .05$), while the remaining variables were not significant (Fig. 2).

3.2. Comparisons of single CT imaging features

The characteristics of the lesion morphologies are shown in Table 2. The positive group patients in the early stage mostly had GGOs (38, 70.4%), a typical imaging manifestation in viral pneumonia, followed by the crazy-paving pattern (16, 29.6%), air bronchogram (14, 25.9%), consolidation (12, 22.2%) and pleural thickening (11, 20.4%). Pulmonary nodules, pleural effusion, lymphadenopathy and pulmonary atelectasis were rare. The presence of GGOs, the crazy-paving pattern, air bronchogram, and pleural thickening was significantly different between the two groups ($P < .05$). The remaining variables were not ($P > .05$).

The lesion distribution characteristics are shown in Table 3. For the positive group, lesions in the early stage were mainly distributed bilaterally (40, 74.1%) and near the pleura (33, 61.1%). The involvement of two lobes and all lobes were most common, seen in 18 (33.3%) and 13 patients (24.1%), respectively. Forty-five patients (83.3%) showed involvement of at least two lobes. Left lower lobe (40, 74.1%) and right lower lobe (43, 79.6%) involvement were also frequently observed. Peripheral, bilateral or lower lung distribution and multilobe involvement was significantly different between the two groups ($P < .05$), and the remaining variables were not significant ($P > .05$).

3.3. Comparisons of combined early CT imaging features

According to the statistical results in Tables 2 and 3, we found that GGOs were the basic manifestation in the positive group. To increase distinguishability on imaging, we combined GGOs with other statistically significant features. Table 4 shows the various combinations of imaging features on early CT. When two features were combined, the

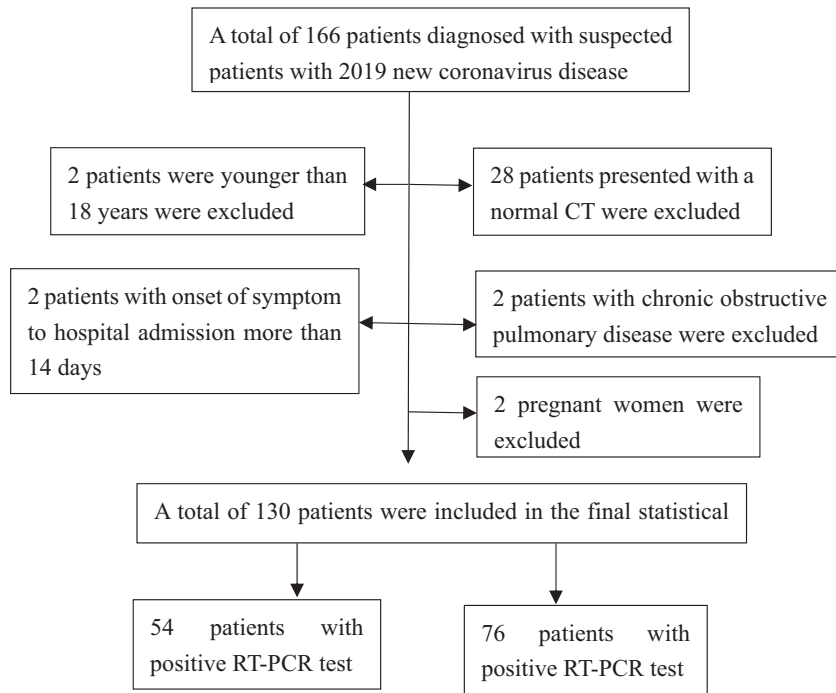


Fig. 1. Flow chart of the study.

combination of GGOs with bilateral pulmonary distribution and the combination of GGOs with pleural distribution were the most common, found in 31 (57.4%) and 30 patients (55.6%), respectively. When three items were combined, 26 patients (48.1%) presented with GGOs and bilateral pulmonary and peripleural distributions. When four items were combined, the combination of GGOs, a bilateral pulmonary distribution, the crazy-paving pattern, and pleural distribution was the most common, seen 12 patients (22.2%). The presence of almost all these combinations was significantly different between the two groups ($P < .05$), except for the combination of GGOs with consolidation.

Table 1
General demographic information.

General information	Positive group <i>n</i> = 54	Negative group <i>n</i> = 76	<i>P</i>
Gender			0.15
Male, n(%)	28(51.9%)	49(64.5%)	
Female, n(%)	26(48.1%)	27(35.5%)	
Age, years	45.1 ± 13.4	41.8 ± 13.6	0.18
Symptoms onset to the first visit, day(s)	4.0(1.0–6.0)	3.0(1.0–5.0)	0.55
Exposure to symptoms onset, day(s)	6.0(3.5–9.5)	5.0(3.0–10.0)	0.90
Epidemiological history			
Patients with Wuhan residence history, n(%)	20(37.0%)	8(10.5%)	<0.01
Patients with Wuhan travel history, n(%)	19(35.2%)	22(28.9%)	0.45
Exposure of South China Seafood Market, n(%)	2(3.7%)	0(0%)	0.17
Contact with patients of fever or COVID-19, n(%)	25(46.3%)	27(35.5%)	0.22
Clustering occurrence, n(%)	24(44.4%)	8(10.5%)	<0.01
History of hypertension, n(%)	7(13.0%)	10(13.2%)	0.97
History of diabetes, n(%)	3(5.6%)	5(6.6%)	1.00
History of cardiovascular disease, n(%)	1(1.9%)	2(2.6%)	1.00
History of cerebrovascular disease, n(%)	1(1.9%)	0(0%)	0.42
History of chronic liver disease, n(%)	0(0%)	3(3.9%)	0.27
History of chronic kidney disease, n(%)	0(0%)	0(0%)	–
History of cancer, n(%)	0(0%)	1(1.3%)	1.00
Smoking, n(%)	11(20.4%)	17(22.4%)	0.79
Drinking, n(%)	8(14.8%)	15(19.7%)	0.47

COVID-19, Corona Virus Disease 2019.

3.4. Comparisons of the diagnostic value of combined imaging features between the positive and negative groups

As shown in Table 5, GGOs with bilateral pulmonary distribution and GGOs with peripleural distribution both presented the highest sensitivity of 57%, followed by GGOs combined with bilateral pulmonary distribution and peripleural distribution at 48%. The remaining combinations had sensitivities of approximately 25%. In contrast, these combinations presented with much better specificity. When combining two items, the specificity of GGOs with the crazy-paving pattern was up to 96%, followed by GGOs with air bronchogram (95%). When three features were combined, the specificity was over 95%, and GGOs with the crazy-paving pattern and bilateral pulmonary distribution had the highest at 99%. The specificity of diagnosis was almost 99% for four items.

4. Discussion

In the positive group, our study showed that GGOs are the basic manifestation in CT imaging of COVID-19, followed by consolidation, the crazy-paving pattern and air bronchogram. Lesions were mainly distributed bilaterally, close to the lower lungs or the pleura. These findings are similar to those in previous descriptive studies on COVID-19 [8,10,13,14] and also overlap with the imaging features of other viral pneumonias. For this reason, we estimated the pathological mechanism of COVID-19 involves transmission through the respiratory tract and damage to the terminal bronchioles and lung parenchyma near the bronchioles in the early stages, which in turn affect the entirety of the lung lobules and results in diffuse alveolar damage, similar to other viral pneumonias [15]. Apparently, the imaging features of COVID-19 greatly resemble those of SARS (severe acute respiratory syndrome) and MERS (Middle East respiratory syndrome), which are other members of the coronavirus family [16–19].

However, some distinguishable imaging features can be seen for COVID-19. The CT imaging features of SARS are mainly manifested by GGOs with consolidation [20]. Lower lung distribution and peripheral involvement are more common, and there is more unifocal involvement

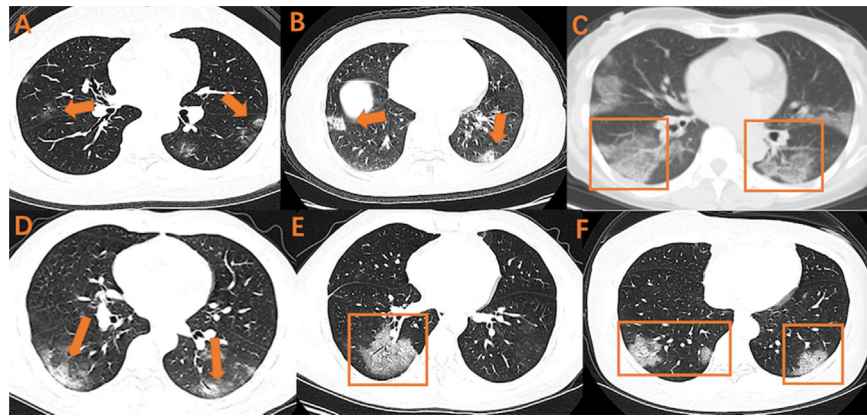


Fig. 2. Various combinations of GGO on early CT imaging GGO, ground glass opacity Various combinations of GGO on early CT imaging were shown as above. A, B, C: GGO with bilateral and subpleural distribution; D: GGO with air bronchogram and bilateral lower pulmonary distribution; E: GGO with air bronchogram; F: GGO with crazy-paving pattern and bilateral lower pulmonary distribution.

than multifocal and bilateral involvement. The manifestations of MERS on chest CT are mainly subpleural distributions, accompanied by extensive GGOs and consolidations [16]. In addition, influenza virus pneumonia has a high frequency of occurrence in winter and spring, with manifestations of cavities, GGOs and a lobular distribution on chest CT [12].

Furthermore, we found that GGOs, the crazy-paving pattern, air bronchogram, and pleural thickening were more common in patients with COVID-19 than in patients with other viral pneumonias on chest CT imaging. Peripheral, bilateral or lower lung distribution and multilobe involvement also presented more frequently in COVID-19 patients. This may help us identify COVID-19 patients with chest CT scans. Previous studies have to date merely described the dynamic changes in the chest CT imaging of COVID-19 and presented the features currently used in the diagnosis of the disease [8,10,13,14,21]. Some of them focused on the sensitivity compared to that of RT-PCR with a relatively small sample size, but they did not compare these features with those of other viral pneumonias or explain how a differential diagnosis could be made by chest CT [9,11]. Our study includes all suspected cases, including positive and negative cases, which may be more useful for early differential diagnosis.

Theoretically, a definite diagnosis cannot be achieved on the basis of one single imaging feature, as it may overlap with individual imaging features from other viral pneumonias as mentioned above. Therefore, we combined several statistically significant imaging features to evaluate the diagnostic value of chest CT scans. Apparently, the combination of features resulted in relatively low sensitivity but extremely high specificity. The average specificity of all combinations was approximately 90%, and the combination of GGOs with the crazy-paving pattern and bilateral pulmonary distribution showed the highest specificity at

99% when three items were combined. The use of a four-item combination also resulted in 99% specificity. In conclusion, the combinations of GGO with different features from chest CT might significantly increase the specificity in the diagnosis of COVID-19. This means that in a series presenting crazy-paving patterns, air bronchograms, bilateral lower pulmonary distributions, bilateral pulmonary distributions and pleural distributions, as long as they appear simultaneously with GGOs on chest CT, COVID-19 should be highly suspected, even if the patient has repeated negative RT-PCR outcomes. This might help emergency physicians identify COVID-19 patients faster and more effectively. Based on accumulated experience, we recommend that these patients be quarantined and have their RT-PCR tests repeated until the average incubation ends, especially in areas with severe outbreaks. Epidemiological exposure, RT-PCR tests and chest CT scans are equally critical to diagnosis.

There are several limitations in our study. First, the goal was to compare the difference in CT imaging features between confirmed and nonconfirmed COVID-19 patients. Some early lesions might not be visible on chest CT since the maximum incubation period is 14 days or even more [6]. Therefore, the expression of time may not be precise enough according to the development of this disease. Second, the current gold standard for the diagnosis of COVID-19 is merely the RT-PCR test [6]. Since the test samples are mostly pharynx swabs rather than bronchoalveolar lavage fluid (BALF) samples, false negative results might still be present after repeat testing.

In summary, the manifestations of COVID-19 vary. Some patients show similar manifestations with those of common viral pneumonias.

Table 2
Lesion morphology in chest CT.

Morphological characteristics	Positive group n = 54	Negative group n = 76	P
GGO	38(70.4%)	32(42.1%)	0.01
Consolidation	12(22.2%)	29(38.2%)	0.05
Crazy-paving pattern	16(29.6%)	3(3.9%)	<0.01
Air bronchogram	14(25.9%)	5(6.6%)	<0.01
Cavitation	1(1.9%)	1(1.3%)	1.00
Pulmonary nodule	8(14.8%)	15(19.7%)	0.47
Lymphadenopathy	4(7.4%)	0(0%)	0.03
Pleural effusion	0(0%)	4(5.3%)	0.14
Pulmonary atelectasis	1(1.9%)	2(2.6%)	1.00
Pleural thickening	11(20.4%)	4(5.3%)	<0.01

GGO, ground glass opacity.

Table 3
Lesion distribution in chest CT.

Distribution characteristics	Positive group n = 54	Negative group n = 76	P
Bilateral pulmonary distribution	40(74.1%)	30(40.8%)	<0.01
Bilateral lower pulmonary distribution	32(59.3%)	19(25.0%)	<0.01
Peripleural distribution	33(61.1%)	21(27.6%)	<0.01
Distribution of lung lobes			
Right upper lobe	26(48.1%)	27(35.5%)	0.15
Right middle lobe	22(40.7%)	23(30.3%)	0.22
Right lower lobe	43(79.6%)	35(46.1%)	<0.01
Left upper lobe	28(51.9%)	31(40.8%)	0.21
Left lower lobe	40(74.1%)	37(48.7%)	<0.01
Number of affected lobes			
Patients of 1 affected lobe	9(16.7%)	37(48.7%)	
Patients of 2 affected lobes	18(33.3%)	15(19.7%)	
Patients of 3 affected lobes	7(13.0%)	13(17.1%)	
Patients of 4 affected lobes	7(13.0%)	1(1.3%)	
Patients of 5 affected lobes	13(24.1%)	10(13.2%)	
Patients of >2 affected lobes	45(83.3%)	39(51.3%)	<0.01

Table 4
Combined CT imaging features between positive group and negative group.

Combined features	Positive group	Negative group	P
	n = 54	n = 76	
GGO + Consolidation	11(20.4%)	8(10.5%)	0.12
GGO+ Crazy-paving pattern	16(29.6%)	3(3.9%)	<0.01
GGO + Air bronchogram	14(15.9%)	4(5.3%)	<0.01
GGO + Bilateral pulmonary distribution	31(57.4%)	15(19.7%)	<0.01
GGO + Bilateral lower pulmonary distribution	21(38.9%)	8(10.5%)	<0.01
GGO + Peripleural distribution	30(55.6%)	16(21.1%)	<0.01
GGO + Bilateral lower pulmonary distribution+Peripleural distribution	17(31.5%)	5(6.6%)	<0.01
GGO + Bilateral pulmonary distribution+Peripleural distribution	26(48.1%)	8(10.5%)	<0.01
GGO + Crazy-paving pattern+Peripleural distribution	12(22.2%)	3(3.9%)	<0.01
GGO + Air bronchogram +Peripleural distribution	11(20.4%)	2(2.6%)	<0.01
GGO + Crazy-paving pattern+Bilateral lower pulmonary distribution	11(20.4%)	1(1.3%)	<0.01
GGO + Air bronchogram+Bilateral lower pulmonary distribution	8(14.8%)	1(1.3%)	<0.01
GGO + Bilateral pulmonary distribution+Crazy-paving Pattern+ Pleural distribution	12(22.2%)	2(2.6%)	<0.01
GGO + bilateral pulmonary distribution+Air bronchogram+ Peripleural distribution	10(18.5%)	1(1.3%)	<0.01
GGO + Bilateral lower pulmonary distribution+Crazy-paving pattern+Peripleural distribution	9(16.7%)	1(1.3%)	<0.01
GGO + Bilateral lower pulmonary distribution+Air bronchogram +Peripleural distribution	6(11.1%)	1(1.3%)	0.02

GGO, ground glass opacity.

However, COVID-19 still demonstrates specific imaging characteristics. The combinations with GGOs could be useful in the identification and differential diagnosis of COVID-19, alerting clinicians to isolate patients for prompt treatment and repeat RT-PCR tests until the incubation period ends.

Credit authorship contribution statement

Congliang Miao: Investigation. **Mengdi Jin:** Writing - original draft. **Li Miao:** Investigation. **Xinying Yang:** Writing - original draft. **Peng Huang:** Investigation. **Huanwen Xiong:** Investigation. **Peijie Huang:** Writing - review & editing. **Qi Zhao:** Writing - review & editing. **Jiang Du:** Conceptualization. **Jiang Hong:** Conceptualization, Writing - review & editing.

Acknowledgements

None.

Table 5

The diagnostic value of combined CT imaging features between positive group and negative group.

Combined features	Sensitivity	Specificity
GGO+ Crazy-paving pattern	0.30	0.96
GGO + Air bronchogram	0.26	0.95
GGO + Bilateral pulmonary distribution	0.57	0.81
GGO + Bilateral lower pulmonary distribution	0.39	0.89
GGO + Peripleural distribution	0.57	0.79
GGO + Bilateral lower pulmonary distribution +Peripleural distribution	0.31	0.93
GGO + Bilateral pulmonary distribution+Peripleural distribution	0.48	0.89
GGO + Crazy-paving pattern+Peripleural distribution	0.22	0.96
GGO + Air bronchogram +Peripleural distribution	0.20	0.97
GGO + Crazy-paving pattern+Bilateral lower pulmonary distribution	0.20	0.99
GGO + Air bronchogram+Bilateral lower pulmonary distribution	0.15	0.99
GGO + Bilateral pulmonary distribution+Crazy-paving Pattern+ Peripleural distribution	0.22	0.97
GGO + bilateral pulmonary distribution+Air bronchogram+ Peripleural distribution	0.19	0.99
GGO + Bilateral lower pulmonary distribution +Crazy-paving pattern+Peripleural distribution	0.17	0.99
GGO + Bilateral lower pulmonary distribution+Air bronchogram +Peripleural distribution	0.11	0.99

GGO, ground glass opacity.

Funding information

This research did not receive any specific grant from funding agencies in the public, commercial, or not-for-profit sectors.

Declaration of competing interest

The authors of this manuscript have no conflicts of interest or relationships with any companies whose products or services may be related to the subject matter of the article.

References

- [1] Lu R, Zhao X, Li J, Niu P, Yang B, Wu H, et al. Genomic characterisation and epidemiology of 2019 novel coronavirus: implications for virus origins and receptor binding. *Lancet* 2020;395(10224):565–74. [https://doi.org/10.1016/S0140-6736\(20\)30251-8](https://doi.org/10.1016/S0140-6736(20)30251-8).
- [2] Lu H, Stratton CW, Tang YW. Outbreak of pneumonia of unknown etiology in Wuhan, China: the mystery and the miracle. *J Med Virol* 2020;92(4):401–2. <https://doi.org/10.1002/jmv.25678>.
- [3] Report of clustering pneumonia of unknown etiology in Wuhan City. <http://wjw.wuhan.gov.cn/front/web/showDetail/2019123108989>.
- [4] Zhu N, Wang W, et al. A novel coronavirus from patients with pneumonia in China. *NEJM* 2019;382(8):727–33. <https://doi.org/10.1056/NEJMoa2001017> [2020].
- [5] Update on the outbreak of new coronavirus pneumonia as of 24:00 on March 17. <http://www.nhc.gov.cn/xcs/yqfkdt/202002/d5e15557ee534fcb5aa9301ea5235f.shtml>.
- [6] Diagnosis and treatment program for COVID-19 (trial version of the 7th edition). <http://www.nhc.gov.cn/yzygj/s7653p/202002/8334a8326dd94d329df351d7da8aefc2/files/b218cfeb1bc54639af227f922bf6b817.pdf>.
- [7] Xie X, Zhong Z, Zhao W, Zheng C, Wang F, Liu J. Chest CT for typical 2019-nCoV pneumonia: relationship to negative RT-PCR testing. *Radiology* 2020;200343. <https://doi.org/10.1148/radiol.2020200343>.
- [8] Chung M, Bernheim A, Mei X, Zhang N, Huang M, Zeng X, et al. CT imaging features of 2019 novel coronavirus (2019-nCoV). *Radiology* 2020;200230(1):202–7. <https://doi.org/10.1148/radiol.2020200230>.
- [9] Fang Y, Zhang H, Xie J, Lin M, Ying L, Pang P, et al. Sensitivity of chest CT for COVID-19: comparison to RT-PCR. *Radiology* 2020;200432. <https://doi.org/10.1148/radiol.2020200432>.
- [10] Kanne JP. Chest CT findings in 2019 novel coronavirus (2019-nCoV) infections from Wuhan, China: key points for the radiologist. *Radiology* 2020;295(1):16–7. <https://doi.org/10.1148/radiol.2020200241>.
- [11] Ai T, Yang Z, Hou H, Zhan C, Chen C, Lv W, et al. Correlation of chest CT and RT-PCR testing in coronavirus disease 2019 (COVID-19) in China: a report of 1014 cases. *Radiology* 2020;200642. <https://doi.org/10.1148/radiol.2020200642>.
- [12] Kim EA, Lee KS, Primack SL, Yoon HK, Byun HS, Kim TS, et al. Viral pneumonias in adults: radiologic and pathologic findings. *Radiographics* 2002;22:S137–49. https://doi.org/10.1148/radiographics.22.suppl_1.g02oc15s137 Spec No.:
- [13] Lei J, Li J, Li X, Qi X. CT imaging of the 2019 novel coronavirus (2019-nCoV) pneumonia. *Radiology* 2020;295(1):18–18. <https://doi.org/10.1148/radiol.2020200236>.
- [14] Shi H, Han X, Zheng C. Evolution of CT manifestations in a patient recovered from 2019 novel coronavirus (2019-nCoV) pneumonia in Wuhan, China. *Radiology* 2020(1):20–20 200269. <https://doi.org/10.1148/radiol.2020200269>.
- [15] Xu Z, Shi L, Wang Y, Zhang J, Huang L, Zhang C, et al. Pathological findings of COVID-19 associated with acute respiratory distress syndrome. *Lancet Respir Med* 2020;8(4):420–2. [https://doi.org/10.1016/S2213-2600\(20\)30076-X](https://doi.org/10.1016/S2213-2600(20)30076-X).

- [16] Ajlan AM, Ahyad RA, Jamjoom LG, Alharthy A, Madani TA. Middle East respiratory syndrome coronavirus (MERS-CoV) infection: chest CT findings. *AJR Am J Roentgenol* 2014;203(4):782–7. <https://doi.org/10.2214/AJR.14.13021>.
- [17] Das KM, Lee EY, Langer RD, Larsson SG. Middle East respiratory syndrome coronavirus: what does a radiologist need to know? *AJR Am J Roentgenol* 2016;206(6):1193–201.
- [18] Wong KT, Antonio GE, Hui DS, Lee N, Yuen EH, Wu A, et al. Thin-section CT of severe acute respiratory syndrome: evaluation of 73 patients exposed to or with the disease. *Radiology* 2003;228(2):395–400. <https://doi.org/10.1148/radiol.2283030541>.
- [19] Zhao D, Ma D, Wang W, Wu H, Yuan C, Jia C, et al. Early X-ray and CT appearances of severe acute respiratory syndrome: an analysis of 28 cases. *Chin Med J (Engl)* 2003;116(6):823–6.
- [20] Koo HJ, Lim S, Choe J, Choi SH, Sung H, Do KH. Radiographic and CT features of viral pneumonia. *Radiographics* 2018;38(3):719–39. <https://doi.org/10.1148/rg.2018170048>.
- [21] Pan F, Ye T, Sun P, Gui S, Liang B, Li L, et al. Time course of lung changes on chest CT during recovery from 2019 novel coronavirus (COVID-19) pneumonia. *Radiology* 2020:200370. <https://doi.org/10.1148/radiol.2020200370>.